Methods for inferring regional surface-mass anomalies from Gravity Recovery and Climate Experiment (GRACE) measurements of time-variable gravity

Sean Swenson and John Wahr

Department of Physics and Cooperative Institute for Research in Environmental Sciences, University of Colorado, Boulder, USA

Received 8 May 2001; revised 9 March 2002; accepted 14 March 2002; published 19 September 2002.

[1] The Gravity Recovery and Climate Experiment, GRACE, will deliver monthly averages of the spherical harmonic coefficients describing the Earth's gravity field, from which we expect to infer time-variable changes in mass, averaged over arbitrary regions having length scales of a few hundred kilometers and larger, to accuracies of better than 1 cm of equivalent water thickness. These data will be useful for examining changes in the distribution of water in the ocean, in snow and ice on polar ice sheets, and in continental water and snow storage. We describe methods of extracting regional mass anomalies from GRACE gravity coefficients. Spatial averaging kernels were created to isolate the gravity signal of individual regions while simultaneously minimizing the effects of GRACE observational errors and contamination from surrounding glacial, hydrological, and oceanic gravity signals. We then estimated the probable accuracy of averaging kernels for regions of arbitrary shape and size. *INDEX TERMS:* 1836 Hydrology: Hydrologic budget (1655); 4283 Oceanography: General: Water masses; 1655 Global Change: Water cycles (1836); 1243 Geodesy and Gravity: Space geodetic surveys; 1640 Global Change: Remote sensing; *KEYWORDS:* GRACE, satellite gravity, hydrology, time-variable gravity, regional water storage

Citation: Swenson, S., and J. Wahr, Methods for inferring regional surface-mass anomalies from Gravity Recovery and Climate Experiment (GRACE) measurements of time-variable gravity, *J. Geophys. Res.*, *107*(B9), 2193, doi:10.1029/2001JB000576, 2002.

1. Introduction

[2] Time-variable gravity changes are caused by a combination of postglacial rebound, fluctuations in atmospheric mass, and the redistribution of water, snow, and ice on land and in the ocean. The spatial resolution of gravity data obtained from satellite measurements has not yet been sufficient to separate the effects of these processes from one another. Data from GRACE, launched in 2002 should provide dramatically improved time-variable gravity measurements. GRACE will deliver monthly averages of the spherical harmonic coefficients describing the Earth's gravity field at scales of a few hundred kilometers and larger.

[3] From the gravity field estimates, we expect to infer time-variable changes in mass, averaged over arbitrary regions having length scales of a few hundred kilometers and larger, to accuracies of better than 1 cm of equivalent water thickness. These data will be useful for examining changes in the distribution of water in the ocean, in snow and ice on polar ice sheets, and in continental water and snow storage. These quantities can then be used to assess and improve climate models, to better understand large-scale hydrological processes, and to monitor the distribution of land-based water for agricultural and water resource applications. Combined with radar altimetry over the oceans, these data can improve estimates of the time-varying ocean heat storage, as well as deep ocean currents. In polar regions, GRACE data can be used to study postglacial rebound and, in conjunction with laser altimetry, to constrain the mass balance of ice sheets.

[4] Because the spatial resolution of GRACE is on the order of a few hundred kilometers, an estimate of a surface-mass anomaly will not be a point measurement, but rather a spatial average. *Wahr et al.* [1998] introduce an averaging method based on a simple Gaussian filter. However, this method does not isolate a specific region. In order to use GRACE to estimate regional changes in surface mass, techniques must be developed which extract regional mass anomalies from GRACE gravity coefficients. In this paper, we describe methods of creating spatial averaging kernels which isolate the gravity signal of individual regions while simultaneously minimizing the effects of GRACE observational errors and the contamination from surrounding glacial, hydrological, and oceanic gravity signals. We then estimate the probable accuracy of averaging kernels for regions of arbitrary shape and size.

2. Inferring Surface Mass Changes From the Time-Variable Gravity Field

[5] It is usual to represent the Earth's gravity field in terms of the shape of the geoid, the equipotential surface that most closely coincides with mean sea level over the ocean. The geoid, N, can be expanded as a sum of

0148-0227/02/2001JB000576$09.00

normalized associated Legendre functions, $\tilde{P}_{lm}$ [see, e.g., *Chao and Gross*, 1987]:

$$N(\theta,\phi) = a\sum_{l=0}^{\infty}\sum_{m=0}^{l}\tilde{P}_{lm}(\cos\theta)\{C_{lm}\cos m\phi + S_{lm}\sin m\phi\} \quad (1)$$

where θ is colatitude, ϕ is longitude, a is the mean radius of the Earth, and C_{lm} and S_{lm} are dimensionless Stokes coefficients. GRACE Project personnel will use the GRACE measurements to solve for the Stokes coefficients up to degree $l \sim 100$ every 30 days, and these coefficients will be made available to users. The spatial scale, λ, associated with a particular Stokes coefficient is inversely proportional to its angular degree, l, and can be found approximately by the relation $\lambda = 20{,}000$ km/l, so that $l \leq 100$ correspond to length scales of $\sim$200 km and larger.

[6] Using these coefficients, it will be possible to infer changes in the gravity field from one 30-day period to the next, and so to study processes involving the redistribution of mass within the Earth and on or above its surface. GRACE will be accurate enough to be sensitive to changes in the Earth's gravity field caused by fluctuations in continental water storage and the polar ice sheets, as well as by changes in atmospheric and oceanic mass distribution. The contributions from the atmosphere can be estimated from independent atmospheric data and largely removed [*Velicogna et al.*, 2001; *Swenson and Wahr*, 2002]. Because most of the remaining sources of time-variable mass change are confined to a thin layer at the Earth's surface, one can approximate the vertically integrated water and ice mass as a surface mass density. With this approximation, *Wahr et al.* [1998] show that a local change in surface mass density, $\Delta\sigma(\theta,\phi)$, can be related to changes in the Stokes coefficients, ΔC_{lm} and ΔS_{lm}, by

$$\Delta\sigma(\theta,\phi) = \frac{a\rho_E}{3}\sum_{l=0}^{\infty}\sum_{m=0}^{l}\frac{(2l+1)}{(1+k_l)}\tilde{P}_{lm}(\cos\theta)\{\Delta C_{lm}\cos m\phi + \Delta S_{lm}\sin m\phi\} \quad (2)$$

where ρ_E is the average density of the solid Earth and k_l are the load love numbers representing the effects of the Earth's response to surface loads. The love numbers can be obtained from *Wahr et al.* [1998].

[7] The Stokes coefficients produced by GRACE will contain measurement errors, $\Delta\delta^c_{lm}$ and $\Delta\delta^s_{lm}$, such that

$$\begin{aligned}\Delta C^{\mathrm{GRACE}}_{lm} &= \Delta C^{\mathrm{true}}_{lm} + \Delta\delta^c_{lm}\\ \Delta S^{\mathrm{GRACE}}_{lm} &= \Delta S^{\mathrm{true}}_{lm} + \Delta\delta^s_{lm}.\end{aligned} \quad (3)$$

Satellite measurement errors include system noise error in the intersatellite range rate, accelerometer error, error in the ultrastable oscillator, and error in the orbits.

[8] If the coefficients of the satellite errors and the surface mass anomaly at n times $t_1, t_2, \ldots t_n$ are uncorrelated for every (l, m) and (l', m'),

$$\begin{aligned}\frac{1}{n}\sum_{i=1}^{n}\Delta C^{\mathrm{true}}_{lm}(t_i)\Delta\delta^c_{l'm'}(t_i) &= \frac{1}{n}\sum_{i=1}^{n}\Delta C^{\mathrm{true}}_{lm}(t_i)\Delta\delta^s_{l'm'}(t_i) = 0\\ \frac{1}{n}\sum_{i=1}^{n}\Delta S^{\mathrm{true}}_{lm}(t_i)\Delta\delta^c_{l'm'}(t_i) &= \frac{1}{n}\sum_{i=1}^{n}\Delta S^{\mathrm{true}}_{lm}(t_i)\Delta\delta^s_{l'm'}(t_i) = 0,\end{aligned} \quad (4)$$

then two terms comprise the expression for the variance of the inferred surface mass anomaly at the point (θ, ϕ):

$$\mathrm{var}(\sigma)^{\mathrm{GRACE}} = \mathrm{var}(\sigma)^{\mathrm{true}} + \mathrm{var}(\sigma)^{\mathrm{sat}}, \quad (5)$$

where the contribution to the variance due to satellite measurement error is

$$\mathrm{var}(\sigma)^{\mathrm{sat}} = \sum_{l,m}\sum_{l',m'}K_lK_{l'}\,\tilde{P}_{lm}(\cos\theta)\,\tilde{P}_{l'm'}(\cos\theta) \quad (6)$$

$$\times\left[\Lambda^{cc}_{ll'mm'}\cos m\phi\cos m'\phi + \Lambda^{cs}_{ll'mm'}\cos m\phi\sin m'\phi + \Lambda^{sc}_{ll'mm'}\sin m\phi\cos m'\phi + \Lambda^{ss}_{ll'mm'}\sin m\phi\sin m'\phi\right]. \quad (7)$$

$$K_l = \frac{a\rho_E}{3}\frac{(2l+1)}{(1+k_l)} \quad (8)$$

converts the geoid coefficients to surface mass coefficients, and $\Lambda_{ll'mm'}$ are the covariance matrices of the GRACE measurement errors. If, for example, the statistical properties of the measurement errors were the same for each of the n months t_i, $i = 1, n$, then

$$\Lambda^{cc}_{ll'mm'} = \frac{1}{n}\sum_{i=1}^{n}\Delta\delta^c_{lm}(t_i)\Delta\delta^c_{l'm'}(t_i), \quad (9)$$

$$\Lambda^{cs}_{ll'mm'} = \frac{1}{n}\sum_{i=1}^{n}\Delta\delta^c_{lm}(t_i)\Delta\delta^s_{l'm'}(t_i), \quad (10)$$

$$\Lambda^{sc}_{ll'mm'} = \frac{1}{n}\sum_{i=1}^{n}\Delta\delta^s_{lm}(t_i)\Delta\delta^c_{l'm'}(t_i), \quad (11)$$

$$\Lambda^{ss}_{ll'mm'} = \frac{1}{n}\sum_{i=1}^{n}\Delta\delta^s_{lm}(t_i)\Delta\delta^s_{l'm'}(t_i). \quad (12)$$

While calculations utilizing the full covariance matrices are outlined in Appendix A, the calculations in this paper are made with certain assumptions which greatly simplify the covariance matrices. First, we assume $\Delta\delta^c_{lm}$ and $\Delta\delta^s_{l'm'}$ are uncorrelated for all values of l, l', m, m'; equations (10) and (11) therefore vanish. Second, we assume $\Delta\delta^c_{lm}$ and $\Delta\delta^c_{l'm'}$ are uncorrelated, and $\Delta\delta^s_{lm}$ and $\Delta\delta^s_{l'm'}$ are uncorrelated, unless $l = l'$ and $m = m'$, so that equations (9) and (12) vanish in those cases. Last, errors are assumed to depend on spatial scale but not orientation; that is, $\Delta\delta^c_{lm} = \Delta\delta^s_{lm}$ and these coefficients depend on l but not m. With these assumptions, equation (7) becomes

$$\mathrm{var}(\sigma)^{\mathrm{sat}} = \sum_{l,m}K_l^2\,B_l^2, \quad (13)$$

where

$$B_l^2 = \frac{1}{n}\sum_{i=1}^{n}\sum_{m=0}^{l}\left[\left(\Delta\delta^c_{lm}(t_i)\right)^2 + \left(\Delta\delta^s_{lm}(t_i)\right)^2\right]. \quad (14)$$

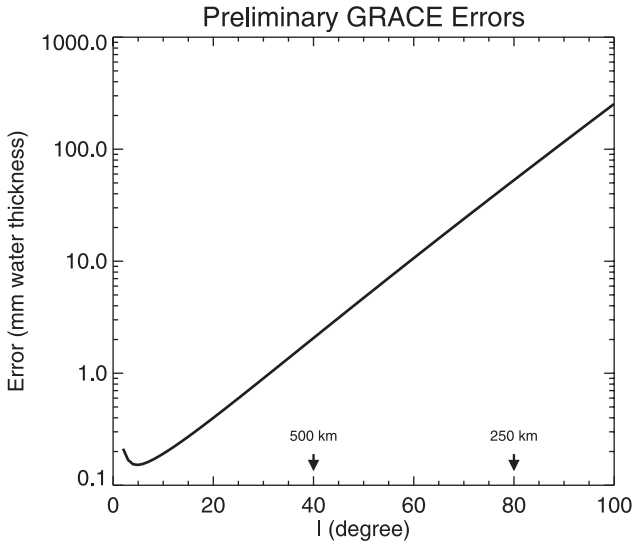

Figure 1. Estimates of the square root of the contribution to the variance of the inferred surface mass anomaly due to GRACE satellite measurement error, as a function of spherical harmonic degree, using equation (13) and values of B_l from B. Thomas and M. Watkins (JPL) consistent with the GRACE SMRD.

Because of our assumptions concerning $\Delta\delta^c_{lm}$ and $\Delta\delta^s_{lm}$ the contribution of the satellite measurement errors to the variance of the surface mass anomaly estimate (equation (13)) is independent of location. B_l are the degree amplitudes of the variance of the satellite errors and describe the contribution of the error at a particular wavelength to the variance of the geoid. In this paper we use preliminary estimates of B_l as a function of l provided by B. Thomas and M. Watkins at the Jet Propulsion Laboratory (personal communication, 1996) that are consistent with those described in *Jet Propulsion Laboratory* [2001].

[9] Figure 1 shows the square root of $\mathrm{var}(\sigma)^{\mathrm{sat}}$ as a function of l. For values of l greater than about 5, the GRACE satellite error estimates increase rapidly with increasing l. In principle, the summations in equations (2) and (13) include contributions from all wavelengths, up to $l = \infty$, and the satellite errors will lead to extremely inaccurate results. Because GRACE will deliver ΔC_{lm} and ΔS_{lm} only to $l \sim 100$, the sums will in practice be truncated at $l_{\mathrm{trnc}} = 100$. Although neglecting the contributions of coefficients with $l > 100$ will reduce the amount of satellite error present in the estimate of $\Delta\sigma(\theta, \phi)$, the error from the larger remaining values of l will still seriously degrade the solutions. In addition, using a truncated sum in equation (2) is not equivalent to a point measurement, $\Delta\sigma(\theta, \phi)$ because it lacks components having length scales less than ~200 km.

[10] These issues can be avoided by averaging $\Delta\sigma(\theta, \phi)$ over a region. Spatial averaging reduces the contributions from large l to the summation in equation (2), reducing the effects of both satellite error and misrepresentation of the gravity field due to the absence of short-wavelength components.

3. Spatial Averaging to Improve Accuracy

[11] The accuracy of estimates of surface mass anomalies can be improved by spatial averaging, at the expense of spatial resolution. An exact averaging kernel, $\vartheta(\theta, \phi)$, is a function which describes the shape of the basin (e.g., a river basin, a region of the ocean floor, an ice sheet, a political boundary) according to

$$\vartheta(\theta,\phi) = \begin{cases} 0 & \text{outside the basin} \\ 1 & \text{inside the basin} \end{cases} \tag{15}$$

The change in vertically integrated water storage averaged over an arbitrary region is

$$\overline{\Delta\sigma}_{\mathrm{region}} = \frac{1}{\Omega_{\mathrm{region}}} \int \Delta\sigma(\theta,\phi)\, \vartheta(\theta,\phi) d\Omega, \tag{16}$$

where $d\Omega = \sin\theta\, d\theta\, d\phi$ is an element of solid angle. Integrating $\vartheta(\theta, \phi)$ over the sphere gives Ω_{region}, the angular area of the region of interest. Using equation (2), equation (16) can be reexpressed by a sum of Stokes coefficients as

$$\overline{\Delta\sigma}_{\mathrm{region}} = \frac{a\,\rho_E}{3\,\Omega_{\mathrm{region}}} \sum_{l=0}^{\infty} \sum_{m=0}^{l} \frac{(2l+1)}{(1+k_l)} \left(\vartheta^c_{lm}\Delta C_{lm} + \vartheta^s_{lm}\Delta S_{lm}\right), \tag{17}$$

where ϑ^c_{lm} and ϑ^s_{lm} are the spherical harmonic coefficients describing $\vartheta(\theta, \phi)$:

$$\vartheta(\theta,\phi) = \frac{1}{4\pi} \sum_{l=0}^{\infty} \sum_{m=0}^{l} \tilde{P}_{lm}(\cos\theta) \left\{\vartheta^c_{lm}\cos m\phi + \vartheta^s_{lm}\sin m\phi\right\} \tag{18}$$

$$\begin{Bmatrix} \vartheta^c_{lm} \\ \vartheta^s_{lm} \end{Bmatrix} = \int \vartheta(\theta,\phi)\tilde{P}_{lm}(\cos\theta) \begin{Bmatrix} \cos m\phi \\ \sin m\phi \end{Bmatrix} d\Omega. \tag{19}$$

One effect of the basin coefficients in equation (17) is to reduce the contribution to $\overline{\Delta\sigma}_{\mathrm{region}}$ from the Stokes coefficients for large l. For example, Figure 2 shows the degree amplitude spectrum,

$$\vartheta_l = \sqrt{\sum_{m=0}^{l} \left[\vartheta^{c\,2}_{lm} + \vartheta^{s\,2}_{lm}\right]}, \tag{20}$$

for disc-shaped basins having radii of 1000, 500, and 100 km. The spectrum has been normalized by dividing by ϑ_0 for each case. As the basin size increases, its degree amplitude is concentrated at relatively smaller l, corresponding to longer wavelengths. Averages over larger regions therefore are influenced less by poorly known short-wavelength signals than are smaller regions.

[12] Basin averages calculated using Stokes coefficients provided by GRACE will differ from the true basin average due to the presence of satellite measurement

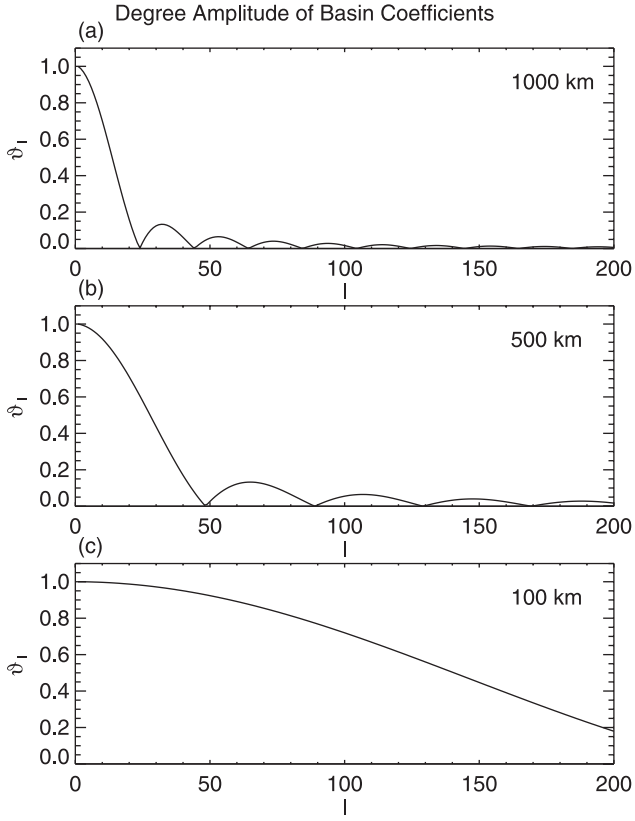

Figure 2. Degree amplitudes of the exact averaging kernels for disc-shaped basins of (a) 1000 km radius, (b) 500 km radius, and (c) 100 km radius. The maximum amplitude has been normalized by $1/\vartheta_0$.

errors and the absence of coefficients for $l > 100$. Failure to include all ϑ^c_{lm} and ϑ^s_{lm} results in an inaccurate representation of the basin shape. Figure 3 shows cross sections of ϑ reconstructed from ϑ^c_{lm} and ϑ^s_{lm} for different values of l_{trnc}, the value of l at which the summation in equation (18) is truncated. The ringing present in these reconstructions near the boundaries of the basin mask, called the Gibbs phenomenon, is due to the absence of basin coefficients with $l > l_{\text{trnc}}$. Ringing increases as l_{trnc} decreases, resulting in a basin average which samples more of the region outside the basin.

[13] With these errors in mind, we write the basin average computed using Stokes coefficients provided by GRACE as the sum of the true basin average, satellite error, and truncation error:

$$\overline{\Delta\sigma}^{\text{GRACE}}_{\text{region}} = \overline{\Delta\sigma}^{\text{true}}_{\text{region}} + \overline{\Delta\sigma}^{\text{satellite error}}_{\text{region}} + \overline{\Delta\sigma}^{\text{truncation error}}_{\text{region}}, \quad (21)$$

where

$$\overline{\Delta\sigma}^{\text{GRACE}}_{\text{region}} = \sum_{l=0}^{l_{\text{trnc}}} \sum_{m=0}^{l} \frac{K_l}{\Omega_{\text{region}}} \left(\vartheta^c_{lm}\Delta C^{\text{GRACE}}_{lm} + \vartheta^s_{lm}\Delta S^{\text{GRACE}}_{lm}\right), \quad (22)$$

$$\overline{\Delta\sigma}^{\text{satellite error}}_{\text{region}} = \sum_{l=0}^{l_{\text{trnc}}} \sum_{m=0}^{l} \frac{K_l}{\Omega_{\text{region}}} \left(\vartheta^c_{lm}\Delta\delta^c_{lm} + \vartheta^s_{lm}\Delta\delta^s_{lm}\right), \quad (23)$$

$$\overline{\Delta\sigma}^{\text{truncation error}}_{\text{region}} = -\sum_{l=l_{\text{trnc}}+1}^{\infty} \sum_{m=0}^{l} \frac{K_l}{\Omega_{\text{region}}} \left(\vartheta^c_{lm}\Delta C^{\text{true}}_{lm} + \vartheta^s_{lm}\Delta S^{\text{true}}_{lm}\right). \quad (24)$$

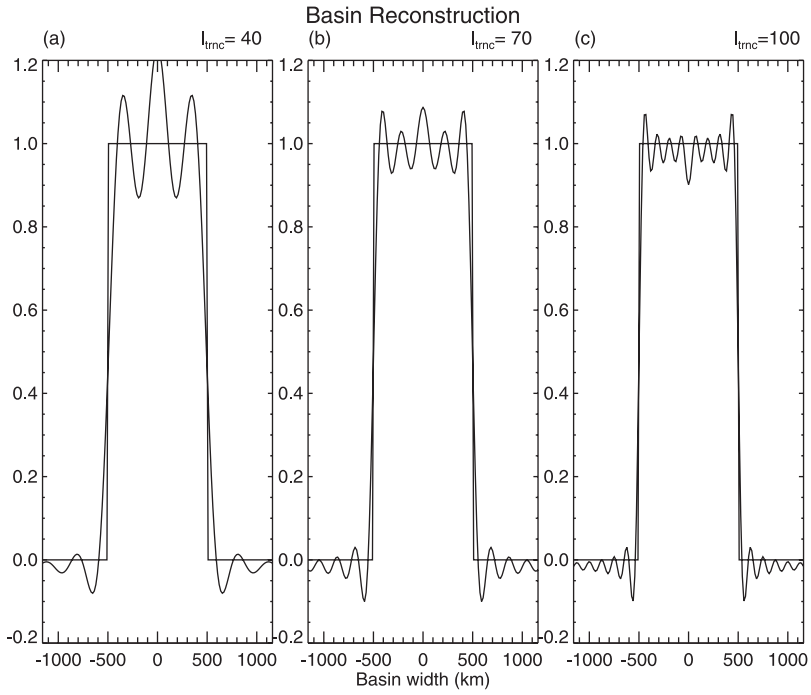

Figure 3. Cross sections of reconstructed basin mask for various values of l_{trnc}.

4. Reducing Satellite Measurement Error

[14] Because GRACE will provide Stokes coefficients only to degree and order ~100, components of surface-mass variability corresponding to $l > 100$ will be absent from the calculation of the basin average. The contribution of high l Stokes coefficients to large basin averages may be unimportant, because, as shown in Figure 2, the basin coefficients become quite small for high l, but as basin size decreases their contribution becomes more significant. In addition to error due to truncation, GRACE data will contain satellite measurement errors. The simplest way to reduce these errors would be to truncate the sum in equation (23) at some $l_{\text{trnc}} < 100$. However, decreasing the value of l_{trnc} increases equation (24), the amount of truncation error. We would like to find a method of decreasing the satellite errors in the estimates of basin-averaged surface mass change without increasing the error due to truncation.

[15] The exact averaging kernel equation (15) changes discontinuously from a value of 1 to 0 at the basin boundaries, resulting in the presence of short-wavelength ϑ^c_{lm} and ϑ^s_{lm} in the expansion of $\vartheta(\theta, \phi)$. Because the satellite errors are greatest at large l, the contribution from these short-wavelength coefficients dominates equation (23), the basin-averaged satellite measurement error. The expansion of an averaging kernel which varies smoothly across the basin boundary has less power in its short-wavelength coefficients than does the exact averaging kernel. However, the basin average computed using a smoothed averaging kernel will less accurately represent the true basin average. This approximate average will be influenced by mass signals outside the basin, referred to as leakage, as well as over- or under-estimating the contribution of the signal inside the basin. While the approximation error cannot be eliminated, we will show that one can create smoothed averaging kernels which produce a reduction in satellite measurement error while keeping the amount of leakage error in the basin-averaged estimates of surface-mass change to an acceptable level for basins having length scales of a few hundred kilometers and larger. We describe two types of averaging kernels. The first kind, described in section 4.1, incorporates a Gaussian filter, and is relatively simple to visualize and compute. The second kind, described in section 4.2, is more complicated but provides a means of minimizing either the leakage error or the satellite measurement error, or the sum of the two.

[16] An approximate basin average can be obtained by replacing the exact averaging kernel, $\vartheta(\theta, \phi)$, by an approximate averaging kernel, $\overline{W}(\theta, \phi)$, in equation (16):

$$\widetilde{\Delta\sigma}_{\text{region}} = \frac{1}{\Omega_{\text{region}}} \int \Delta\sigma(\theta,\phi)\overline{W}(\theta,\phi)\, d\Omega, \tag{25}$$

where $\widetilde{\Delta\sigma}_{region}$ denotes the approximate basin average. Expanding $\overline{W}$ as

$$\overline{W}(\theta,\phi) = \frac{1}{4\pi} \sum_{l=0}^{l_{\text{trnc}}} \sum_{m=0}^{l} \tilde{P}_{lm}(\cos\theta)\left\{W^c_{lm}\cos m\phi + W^s_{lm}\sin m\phi\right\}, \tag{26}$$

the approximate basin average can be expressed in terms of Stokes coefficients as

$$\widetilde{\Delta\sigma}_{\text{region}} = \sum_{l,m} \frac{K_l}{\Omega_{\text{region}}} \left(W^c_{lm}\Delta C_{lm} + W^s_{lm}\Delta S_{lm}\right). \tag{27}$$

When computed using this approximate averaging kernel, the contribution of satellite measurement error to the variance of the average surface mass anomaly becomes

$$\text{var}(\varepsilon_{sat}) = \frac{1}{\Omega^2_{\text{region}}} \sum_{l,m} \frac{K_l^2\, B_l^2}{2l+1} \left[W^{c\,2}_{lm} + W^{s\,2}_{lm}\right]. \tag{28}$$

4.1. Gaussian Smoothing

[17] A smooth averaging kernel, $\overline{W}(\theta, \phi)$, may be created in a straightforward way by convolving the basin function, $\vartheta(\theta, \phi)$, with a Gaussian filter:

$$\overline{W}(\theta,\phi) = \int W(\theta,\phi,\theta',\phi')\,\vartheta(\theta',\phi')\, d\Omega', \tag{29}$$

where equation (29) is integrated over solid angle and, following *Jekeli* [1981], the Gaussian filter, $W(\theta, \phi, \theta', \phi')$, depends only on the angle γ between two points (θ, ϕ) and (θ', ϕ'), i.e., $\cos\gamma = \cos\theta\cos\theta' + \sin\theta\sin\theta'\cos(\phi - \phi')$,

$$W(\theta,\phi,\theta',\phi') = W(\gamma) = \frac{b}{2\pi}\frac{\exp[-b(1-\cos\gamma)]}{1-e^{-2b}}, \tag{30}$$

$$b = \frac{\ln(2)}{\left(1-\cos\left(r_{\frac{1}{2}}/a\right)\right)}. \tag{31}$$

$r_{\frac{1}{2}}/a$ is the half width of the Gaussian smoothing function; when $\gamma = r_{\frac{1}{2}}/a$, $W(\gamma) = 12W(0)$. The new averaging kernel, $\overline{W}$, changes smoothly from a value of 1 inside the boundary to a value of 0 outside the boundary over a horizontal distance of approximately $r_{\frac{1}{2}}$. For this type of averaging kernel, the weighting coefficients in (26) are defined according to

$$\begin{Bmatrix} W^c_{lm} \\ W^s_{lm} \end{Bmatrix} = 2\pi\, W_l \begin{Bmatrix} \vartheta^c_{lm} \\ \vartheta^s_{lm} \end{Bmatrix}, \tag{32}$$

where

$$W_l = \frac{1}{\sqrt{2l+1}} \int_0^{\pi} W(\gamma)\, \tilde{P}_{l0}(\cos\gamma)\sin\gamma\, d\gamma. \tag{33}$$

W_l may be computed recursively by the following relation:

$$\begin{aligned} W_0 &= \frac{1}{2\pi}, \\ W_1 &= \frac{1}{2\pi}\left[\frac{1+e^{-2b}}{1-e^{-2b}} - \frac{1}{b}\right], \\ W_{l+1} &= -\frac{2l+1}{b}W_l + W_{l-1} \end{aligned} \tag{34}$$

[18] Figure 4 shows the result of using a Gaussian filter to smooth the exact averaging kernel, in this case that of the Missouri river basin. Changing the half width of the Gaussian filter allows one to control the relative amounts

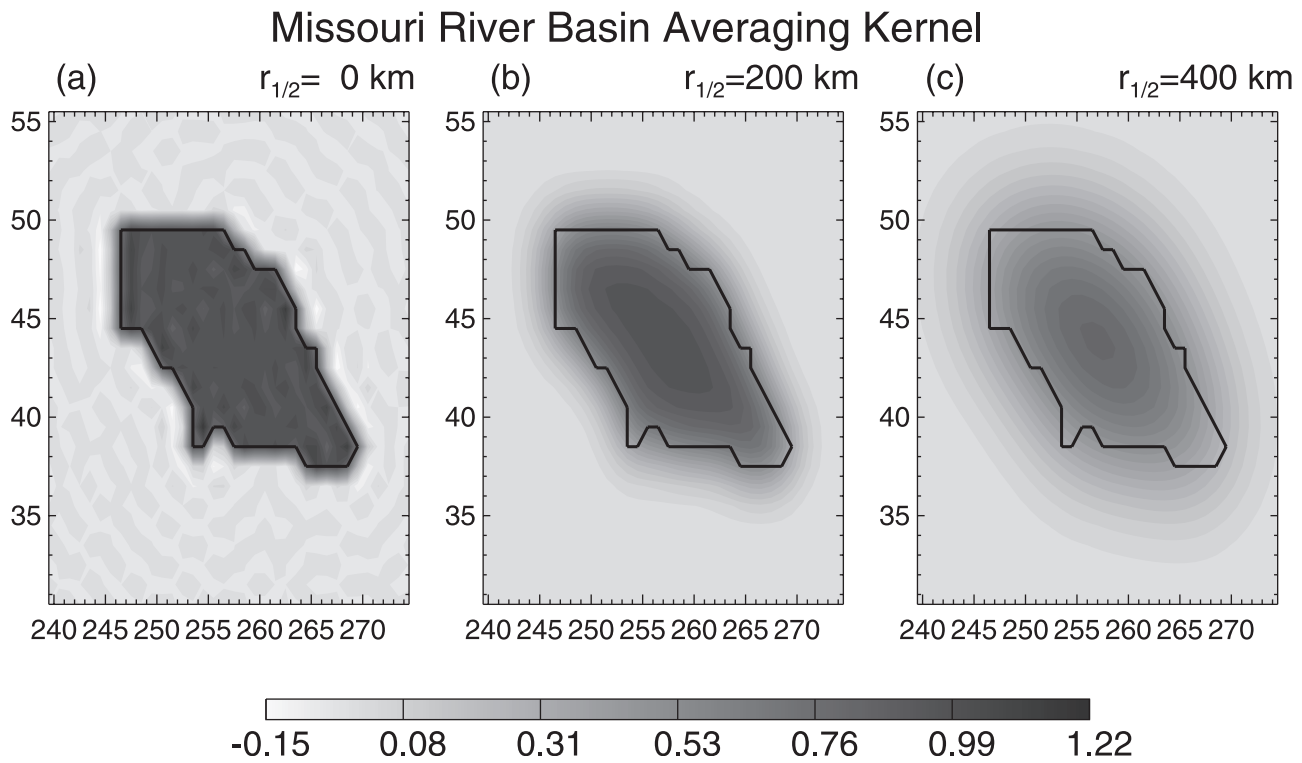

Figure 4. Examples of changing the half width of the Gaussian filter used to smooth the basin mask.

of satellite and leakage error. Small values of $r_{\frac{1}{2}}/a$ lead to an approximate averaging kernel which changes rapidly at its boundaries; the weighting coefficients therefore contain power at short-wavelengths and the error budget is dominated by satellite error. Large values of $r_{\frac{1}{2}}/a$ reduce the amplitude of the short-wavelength weighting coefficients, but increase the amount of error due to leakage from regions surrounding the basin of interest.

[19] Figure 4a shows the exact averaging kernel. It has a value of 1 inside the basin and 0 outside the basin. As previously noted, the ringing at the boundaries is due to the finite upper limit ($l_{\mathrm{trnc}} = 100$) in the summation in equation (26) used to calculate $\overline{W}(\theta, \phi)$. Figures 4b and 4c show the effects of smoothing using 200 and 400 km Gaussian filters, respectively. At 200 km, the averaging kernel changes continuously across the basin edge, while at the same time nearly reproducing the basin shape. When a 400 km filter is applied, the averaging kernel becomes much smoother than that in Figure 4b and samples a larger portion of the surrounding regions.

4.2. Optimizing the Averaging Kernel

[20] While smoothing the exact averaging kernel with a Gaussian filter provides a simple and intuitive way of creating an averaging kernel with decreased short-wavelength components, it may not provide the most accurate estimate of the basin average. We outline two minimization techniques which incorporate measures of satellite and leakage errors to create an optimal averaging kernel. In the first case we minimize the sum of the satellite and leakage errors, while in the second case we fix one type of error to a specific value and minimize the other type.

[21] If ϑ is the exact averaging kernel, then the total approximation error, or leakage, in our estimate of the mass anomaly of the basin at time t_i is the difference between equations (16) and (25):

$$\varepsilon(t_i) = \int \left[\overline{W}(\theta,\phi) - \vartheta(\theta,\phi)\right]\, \sigma(\theta,\phi,t_i)\, d\Omega. \tag{35}$$

The variance of the leakage is then

$$\begin{aligned}\mathrm{var}(\varepsilon_{lkg}) &= \frac{1}{n}\sum_{i=1}^{n}\left[\varepsilon(t_i)\right]^2 \\ &= \int \left[\overline{W}(\theta,\phi) - \vartheta(\theta,\phi)\right]\left[\overline{W}(\theta',\phi') - \vartheta(\theta',\phi')\right] \\ &\quad \cdot \left[\frac{1}{n}\sum_{i=1}^{n}\sigma(\theta,\phi,t_i)\sigma(\theta',\phi',t_i)\right] d\Omega\, d\Omega'.\end{aligned} \tag{36}$$

While the construction of an optimal averaging kernel can incorporate a signal covariance function having any angular dependence (described in Appendix A), the expression for $\mathrm{var}(\varepsilon_{lkg})$ is greatly simplified if we assume that there exists a correlation which depends only on the angular distance, α, between (θ, ϕ) and (θ', ϕ'), so that

$$\frac{1}{n}\sum_{i=1}^{n}\sigma(\theta,\phi,t_i)\, \sigma(\theta',\phi',t_i) = \sigma_0^2\, G(\alpha), \tag{37}$$

where σ_0^2, the variance of the surface mass signal at any point, is assumed to be uniform over the basin and its surroundings, and $G(\alpha)$ is an appropriate function for describing the correlation (in section 5, $G(\alpha)$ will be chosen to be a Gaussian function of α). Replacing $\overline{W}$ and ϑ with

their respective spherical harmonic expansions, the variance of the basin average leakage becomes

$$\mathrm{var}(\varepsilon_{lkg}) = \frac{\sigma_0^2}{\Omega^2_{\mathrm{region}}} \sum_{l=0}^{\infty} \sum_{m=0}^{l} \frac{G_l}{2} \left[\left(W^c_{lm} - \vartheta^c_{lm}\right)^2 + \left(W^s_{lm} - \vartheta^s_{lm}\right)^2 \right], \tag{38}$$

where

$$G_l = \int G(\alpha) P_l(\cos\alpha)\, \sin\alpha\, d\alpha. \tag{39}$$

4.2.1. Minimization of total error

[22] To find averaging kernel coefficients which minimize the total error, we set the partial derivatives with respect to W^c_{lm} and W^s_{lm} of the sum of the error variances to zero,

$$\frac{\partial}{\partial W^{c,s}_{lm}} \left\{ \mathrm{var}(\varepsilon_{\mathrm{sat}}) + \mathrm{var}\left(\varepsilon_{lkg}\right) \right\} = 0, \tag{40}$$

which produces the following set of equations:

$$\left\{ \begin{array}{c} W^c_{lm} \\ W^s_{lm} \end{array} \right\} = \left[1 + \frac{2\, K_l^2\, B_l^2}{\sigma_0^2\, G_l\, (2l+1)} \right]^{-1} \left\{ \begin{array}{c} \vartheta^c_{lm} \\ \vartheta^s_{lm} \end{array} \right\}. \tag{41}$$

Equation (41) makes it possible to find optimal averaging coefficients for a specific basin, from knowledge of the signal variance (σ_0^2), the signal correlation function (G_l) and the degree variances of the GRACE measurement errors (B_l^2).

4.2.2. Lagrange multiplier method

[23] While the previous method fulfills the goal of minimizing the total error, it requires *a priori* estimates of both the amplitude and angular dependence of the covariance function to do so. If these estimates are unavailable or unreliable, it may desirable to create an averaging kernel which does not depend on a foreknowledge of the signal characteristics. An alternative definition of leakage, independent of the signal, is the ratio of the spatial variance of the difference between the exact and approximate averaging kernels to that of the exact averaging kernel,

$$\begin{aligned} \mathrm{var}(\varepsilon_{lkg}) &= \frac{\int \left[\overline{W}(\theta,\phi) - \vartheta(\theta,\phi)\right]^2\, d\Omega}{\int \left[\vartheta(\theta,\phi)\right]^2\, d\Omega} \\ &= \frac{1}{4\pi\Omega_{\mathrm{region}}} \sum_{l,m} \left[\left(W^c_{lm} - \vartheta^c_{lm}\right)^2 + \left(W^s_{lm} - \vartheta^s_{lm}\right)^2 \right] \end{aligned} \tag{42}$$

One may use the method of Lagrange multipliers to create an averaging kernel which minimizes this leakage error subject to a constraint on the value of satellite measurement error. Let δ^2 be the desired variance of the average satellite measurement error equation (28) and let $\Delta^2 = \delta^2\, \Omega^2_{\mathrm{region}}$ Denoting the Lagrange multiplier by λ, we determine the values of W^c_{lm}, W^s_{lm}, and λ that minimize the quantity

$$\begin{aligned} \xi = &\sum_{l,m} \left\{ \left[W^c_{lm} - \vartheta^c_{lm}\right]^2 + \left[W^s_{lm} - \vartheta^s_{lm}\right]^2 \right\} \\ &+ \lambda \left\{ \sum_{l,m} \frac{K_l^2\, B_l^2}{2l+1} \left[W^{c\,2}_{lm} + W^{s\,2}_{lm} \right] - \Delta^2 \right\}, \end{aligned} \tag{43}$$

where we have absorbed the $4\pi\Omega_{\mathrm{region}}$ in equation (42) into λ. Setting the partial derivatives of ξ with respect to W_{clm} and W_{slm} equal to zero gives the set of equations

$$\left\{ \begin{array}{c} W^c_{lm} \\ W^s_{lm} \end{array} \right\} = \left[1 + \lambda \frac{K_l^2\, B_l^2}{2l+1} \right]^{-1} \left\{ \begin{array}{c} \vartheta^c_{lm} \\ \vartheta^s_{lm} \end{array} \right\}. \tag{44}$$

Setting the partial derivative of ξ with respect to λ equal to zero returns the requirement that the effects of the satellite measurement error be equal to Δ^2:

$$\sum_{l,m} \frac{K_l^2\, B_l^2}{2l+1} \left[W^{c\,2}_{lm} + W^{s\,2}_{lm} \right] = \Delta^2, \tag{45}$$

which can be combined with (44) to give an equation for λ

$$\sum_{l,m} \frac{K_l^2\, B_l^2}{2l+1} \frac{\vartheta^{c\,2}_{lm} + \vartheta^{s\,2}_{lm}}{\left[1 + \lambda \frac{K_l^2\, B_l^2}{2l+1} \right]^2} = \Delta^2. \tag{46}$$

Once λ is determined from equation (46), it can be used in equation (44) to solve for W^c_{lm} and W^s_{lm}. In general, there are approximately l^2_{trnc} values of λ which are solutions to equation (46). However, there exists only one solution which is positive, and it is this root which provides the true leakage minimum; the negative roots are only local extrema. If one inadvertently specifies a value for Δ^2 which is greater than that obtained by using the exact averaging kernel coefficients, ϑ^c_{lm} and ϑ^s_{lm} in equation (28), then no positive roots of equation (46) exist.

[24] To create an averaging kernel which fixes the leakage error (42) to a specific value while minimizing the satellite error, one still uses equation (44). λ, however, is determined from

$$\sum_{l,m} \left(\vartheta^{c\,2}_{lm} + \vartheta^{s\,2}_{lm} \right) \left[\frac{1}{1 + \lambda\, \frac{K_l^2\, B_l^2}{2l+1}} - 1 \right]^2 = R\, 4\pi\Omega_{\mathrm{region}}, \tag{47}$$

where R is the desired leakage ratio defined in equation (42).

5. Gaussian Smoothing Versus Minimization

[25] To assess the probable accuracies of the approximate averaging kernels, we first examine the one-dimensional case of a disc-shaped basin. To compute the leakage error, one requires an estimate of the length scale, d, of the spatial correlation of the surface-mass change signal. One source of surface-mass variability is terrestrial water storage. While surface water, snow water, and groundwater are all sources of water storage variability, *Rodell and Famiglietti* [2001] determined that the largest component of variability in the American Midwest is soil moisture. We assume that this relationship characterizes all of the basins examined in this study. Studies such as *Entin et al.* [2000], *Vinnikov et al.* [1996], and *Cayan and Georgakakos* [1995] have shown the spatial coherence of soil moisture to have a length scale ranging from 200 to 800 km. While *Entin et al.* [2000] employ a covariance function which decays exponentially

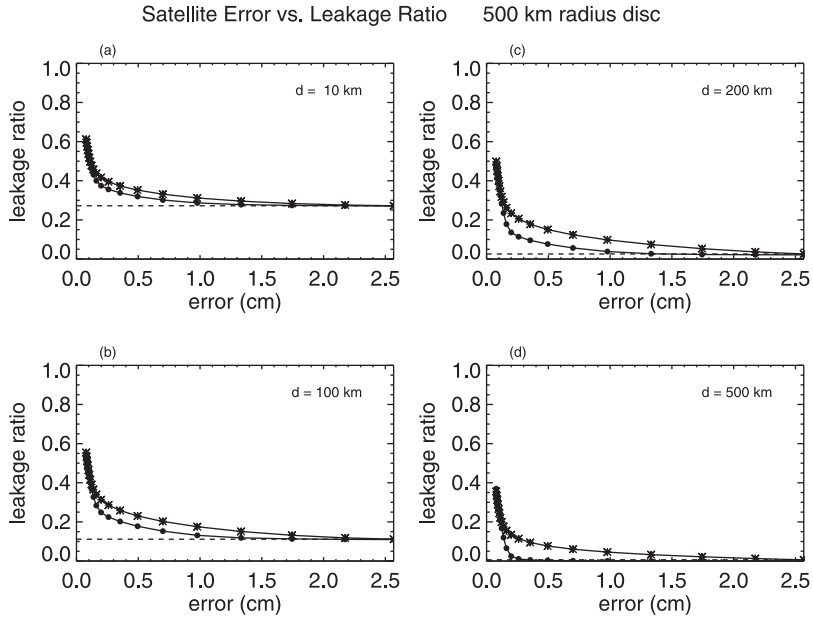

Figure 5. Leakage as a function of the specified RMS of the satellite measurement error, Δ, for a disc-shaped, 500 km radius basin for different surface-mass anomaly correlation lengths, d. Dots denote the Lagrange multplier minimization method, and asterisks denote the Gaussian smoothing method. (a) d = 10 km, (b) 100 km, (c) 200 km, and (d) 500 km. Dashed line represents truncation error.

with distance, we have chosen to use a Gaussian distribution (equation (30)) to describe the correlation between surface-mass variability at different locations. This assumption is based on the ease of manipulation of the Gaussian function in the spherical harmonic domain. In this case, the coefficients G_l, of the spatial covariance function (equation (37)) are computed in the same manner as the smoothing coefficients W_l, using the recursion relation (34) where d, the spatial correlation length scale, replaces $r_{\frac{1}{2}}$.

[26] To compare the Gaussian smoothing process to the minimization process, we first create Gaussian kernels for disc-shaped basins with filters of various half widths. For each kernel, we compute the satellite error using equation (28). Next, we use the Lagrange multiplier method to create an optimal averaging kernel for that value of satellite error, and compare the leakage ratios for the two types of averaging kernel. We define the leakage ratio, R_{lkg}, as the square root of the ratio of the variance of the error caused by

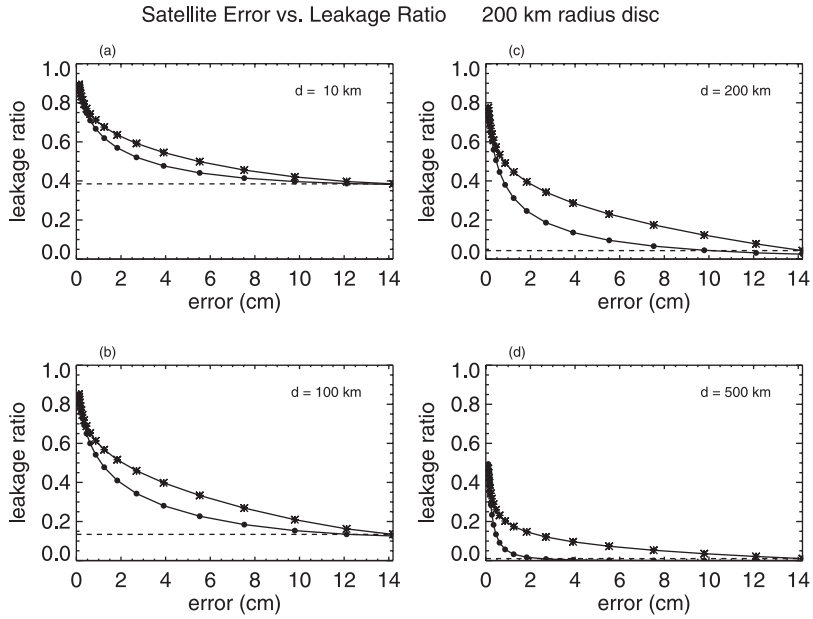

Figure 6. Same as Figure 5, but for a disc-shaped basin having a radius of 200 km.

the approximate averaging kernel to the variance of the true basin-averaged signal. R_{lkg} is thus independent of the amplitude of the covariance function. Because the leakage contains the effects of both the approximate averaging kernel and the finite upper limit in the summations in the expressions for the basin averages, we split the sum in equation (42) at l_{trnc}. Dividing by the expression for the correct surface-mass variance gives

$$R_{lkg}^2 = \frac{\sum_{l=0}^{l_{\text{trnc}}} \sum_{m=0}^{l} G_l \left[\left(W_{lm}^c - \vartheta_{lm}^c \right)^2 + \left(W_{lm}^s - \vartheta_{lm}^s \right)^2 \right]}{\sum_{l=0}^{\infty} \sum_{m=0}^{l} G_l \left[\vartheta_{lm}^{c\,2} + \vartheta_{lm}^{s\,2} \right]} + \frac{\sum_{l=l_{\text{trnc}}+1}^{\infty} \sum_{m=0}^{l} G_l \left[\vartheta_{lm}^{c\,2} + \vartheta_{lm}^{s\,2} \right]}{\sum_{l=0}^{\infty} \sum_{m=0}^{l} G_l \left[\vartheta_{lm}^{c\,2} + \vartheta_{lm}^{s\,2} \right]}. \quad (48)$$

The first term on the right-hand side of equation (48) describes the approximation error made by replacing the true basin function, $\vartheta(\theta, \phi)$, by the approximate averaging kernel, $\overline{W}(\theta, \phi)$. In this paper we assume GRACE will only supply Stokes coefficients to degree $l_{\text{trnc}} = 100$. The second term describes the truncation error due to neglecting terms $l > 100$ when calculating the basin average. While the approximation error depends on the form of a particular averaging kernel, the truncation error has a constant value fixed by the value of l_{trnc} and, through the G_l, the value of d. The maximum value of satellite error for a given basin shape can be found by setting w_{lm}^c and w_{lm}^s to ϑ_{lm}^c and ϑ_{lm}^s in (28) when solving for $\text{var}(\varepsilon_{\text{sat}})$. The exact averaging kernel, ϑ, has an additional property: because its approximation error is identically zero, its leakage ratio is entirely due to truncation error. Figure 5 shows the leakage ratio as a function of satellite error and spatial correlation scale of the signal, d, for a 500 km radius, disc-shaped basin. The level of truncation error can be seen in Figure 5 as the value taken by R_{lkg} as the satellite error approaches its maximum value (dashed line). From Figure 5a it can be seen that when surface-mass anomalies are correlated to about 10 km, truncation error is about 30% of the signal variance, and dominates R_{lkg} for satellite errors greater than about 3 mm. As the signal correlation length, d, increases, the amplitude of the short-wavelength components of the surface-mass signal decrease, and therefore the truncation error decreases. As the truncation error diminishes, the difference between the minimization method and the Gaussian smoothing method becomes more apparent. For example, the leakage due to the Gaussian method at 1 cm satellite error and 200 km correlation length is almost double that due to the minimization method. The effectiveness of the minimization method in reducing leakage error is even more pronounced in the case of a 200 km radius disc (Figure 6).

[27] Figure 7 shows the reconstructed cross sections of the Gaussian and optimal averaging kernels designed to produce a satellite error of 1 cm for two disc-shaped basins. Each plot assumes a correlation length, d, of 200 km. Figure 7a shows a 500 km disc. In order to achieve a 1 cm satellite error, the Gaussian averaging kernel has a roll-off, $r_{\frac{1}{2}}$, of 125 km. A visual comparison of the two averaging kernels confirms Figure 5c; the optimal kernel more closely resembles the truncated basin shape (dashed line) and therefore produces less leakage than the Gaussian averaging kernel. The truncated basin shape lacks the short-wavelength components needed to reproduce the exact basin shape (solid line), but because the correlation length is sufficiently large, the component of R_{lkg} due to truncation error is $\ll 1$.

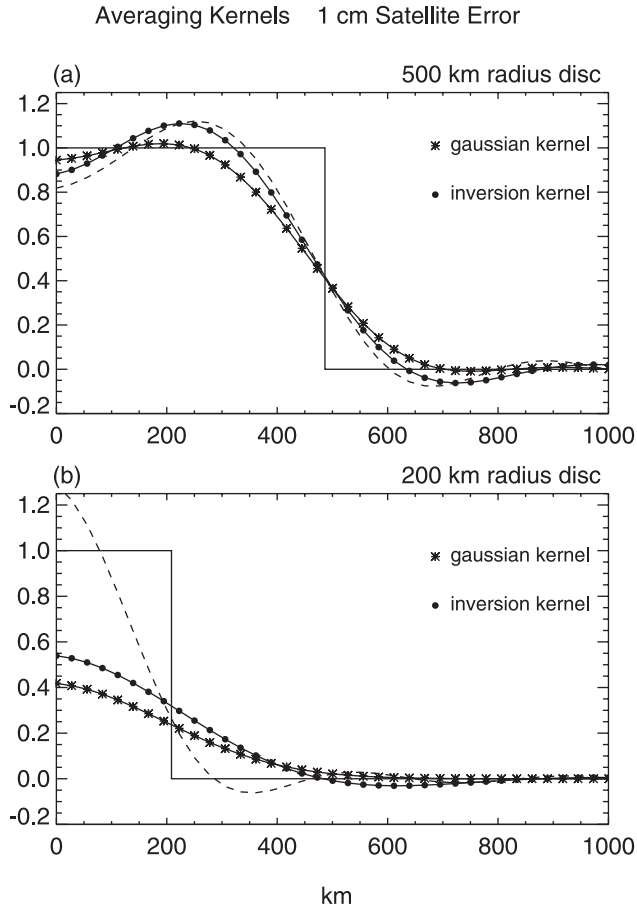

Figure 7. Cross sections of averaging kernels for (a) a 500 km radius basin and (b) a 200 km radius basin. The solid line represents the true basin shape, and the dashed line represents the basin shape computed using only basin coefficients of $l \leq l_{\text{trnc}}$. The surface-mass anomaly correlation length is $d = 200$ km. The averaging functions are computed so that the RMS mass error due to the satellite measurement error is 1 cm in each case.

[28] Figure 7b shows a 200 km disc. The Gaussian averaging kernel in this case employs a roll-off of 215 km to produce the required 1 cm satellite error. Again, the truncated basin shape does not well represent the exact basin shape, but Figure 6c shows the truncation error component to be <5%. However, the leakage is greater than for the 500 km disc because neither averaging kernel closely resembles the truncated basin shape. At 1 cm satellite error, the leakage ratio in Figure 6c is nearly 0.5. This large approximation error is due to the smoothness in the averaging kernels required by the condition that the satellite error must be 1 cm.

6. Comparison With Real Drainage Basins

[29] While the calculations in the previous section employ disc-shaped basins in order to better understand

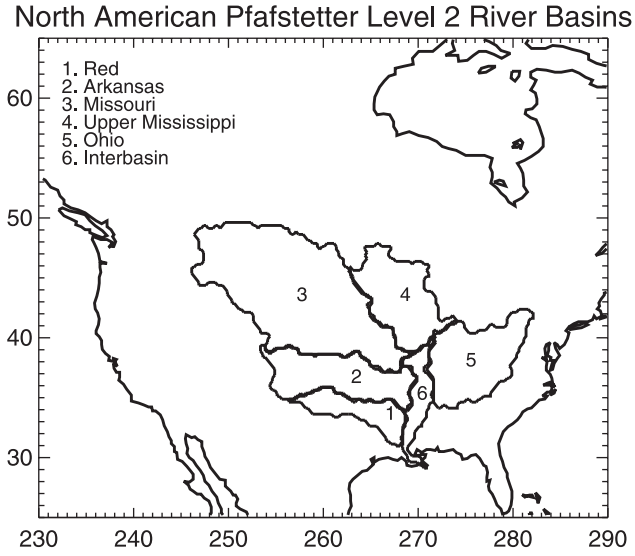

Figure 8. North American river basins.

the effectiveness of each of the averaging kernels, a real basin, whether it describes an oceanic region, a polar ice stream, a river basin, or a political boundary, is rarely shaped so simply. For six North American river basins (Figure 8) of varying shapes and sizes, we calculate the average satellite and leakage errors for each basin using the Gaussian smoothing method and the Lagrange multiplier method. The river basin masks were extracted from the HYDRO 1K Elevation Derivative Database maintained by the U.S. Geological Survey EROS Data Center.

[30] For a basin average with 1 cm satellite error, leakage ratios obtained using a Gaussian averaging kernel range from approximately 0.4 for the smallest basin (220,000 km^2 in area) to 0.1 for the largest basin (1,400,000 km^2 in area) for a correlation length of 200 km (Figure 9). Leakage ratios for the minimization method are about half this amount, ranging from 0.2 to 0.05. Taking 4 cm as a typical value for the RMS variation in midlatitude soil moisture [*Entin et al.*, 2000, Table 1], one would then expect leakage due to the use of the Gaussian averaging kernel to account for about

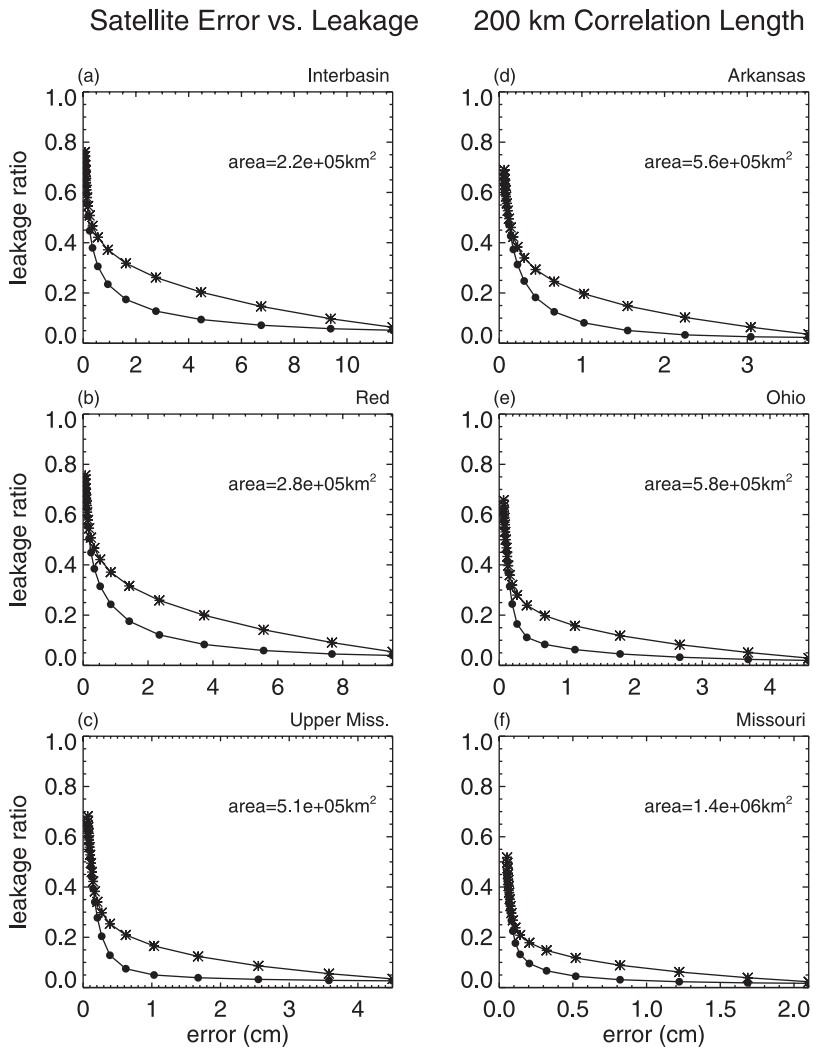

Figure 9. Leakage as a function of RMS satellite measurement error for six North American river basins. *d*, the surface-mass anomaly correlation length, is 200 km. Dots denote the Lagrange multiplier minimization method and asterisks denote the Gaussian smoothing method. (a) Interbasin, (b) Red River, (c) Upper Mississippi River, (d) Arkansas River, (e) Ohio River, and (f) Missouri River.

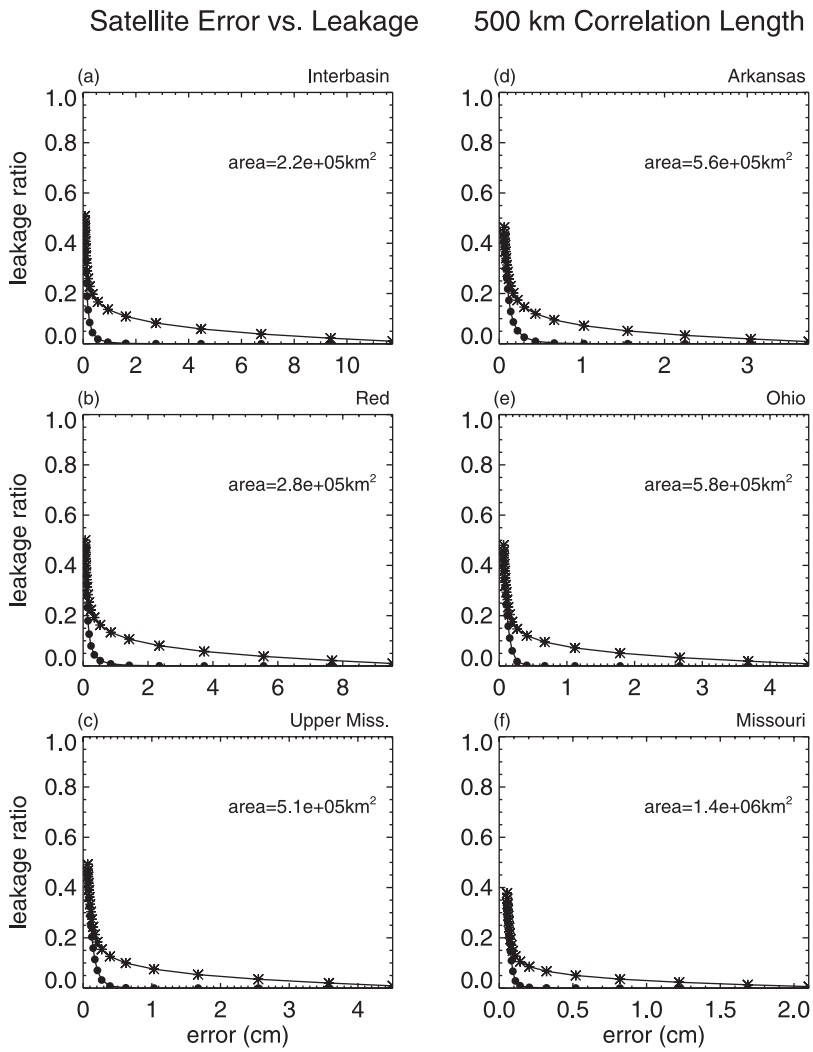

Figure 10. Same as Figure 9, but for a surface-mass anomaly correlation length, d, of 500 km.

1.6 cm of error for basin (Figure 9a) and 0.4 cm of error for basin (Figure 9f). Use of the minimization method would reduce the leakage to approximately 0.8 cm for basin (Figure 9a) and 0.2 cm for basin (Figure 9f). If the correlation length of soil moisture variability is 500 km (Figure 10), the leakage ratio for a basin with 1 cm satellite error ranges from about 0.2 for the smallest basin to less than 0.05 for the largest basin when the Gaussian smoothing method is used. Applying the optimal kernel results in leakage errors which are negligible for even the smallest of these basins. In this case, one could set the satellite error to as low as 0.2 cm without producing a significant amount of leakage in the basin averaged estimates of surface mass variability.

7. Summary

[31] GRACE, scheduled for launch in 2002, will deliver monthly averages of the Earth's geoid, in the form of Stokes coefficients. The finite number of Stokes coefficients provided by GRACE prohibits the estimation of surface mass anomalies at a point, but regional averages can be made. Because the expected satellite measurement errors increase rapidly for short wavelengths, an average calculated using the exact representation of the basin shape, the spectrum of which has power at all wavelengths, is influenced by all the errors associated with these gravity data. A smooth averaging kernel contains less power at short wavelengths, and its use in computing basin averages will lead to a smaller satellite error. However, any approximate averaging kernel will no longer exactly sample the region of interest, and signals from surrounding areas will leak into the estimate of the basin average.

[32] We have outlined different methods for creating approximate averaging kernels which extract the average surface-mass anomaly of a desired region from the GRACE geoid coefficients. Each of these methods reduce the amount of satellite error present in the basin average. One method uses a Gaussian filter (30) to smooth the exact averaging kernel (equation (15)), providing a conceptually and computationally simple means of creating a new averaging kernel. In this case, W_{lm}^{c} and W_{lm}^{s} used in equation (27), are given by equations (32)–(34). However, tuning the width of the Gaussian filter to change the amount of satellite error in the average requires a certain

amount of trial-and-error. In addition, the leakage introduced by this smoothed averaging kernel may not be minimized.

[33] Two minimization techniques for finding W^c_{lm} and W^s_{lm} were outlined, one of which created an averaging kernel which minimized the total error (equation (41)). The other technique used a Lagrange multiplier (equation (44)). The Lagrange multiplier, λ, either minimized the leakage for a given value of satellite error (equation (46)) or minimized the satellite error for a given leakage level (equation (47)). Both methods, described in Appendix A, can incorporate the full covariance matrices of satellite error and/or expected signal. Full satellite error covariance matrices will be provided by GRACE Project personnel when the Stokes coefficients are made available to users. A priori signal covariance matrices may be obtainable from hydrological models or other data sets. However, both minimization techniques simplify considerably under the assumption of azimuthal symmetry.

[34] The method for developing weighting coefficients derived by minimizing the equations describing the total error requires an a priori description of the expected signal covariance. Because of the additional complexities of analyzing these data, we will assess this method in further studies. Instead, we used a Lagrange multiplier method to create averaging kernels which were optimized without the use of an expected signal variability. The Lagrange multiplier minimization method is somewhat more complicated than applying a Gaussian filter, but it decreases the leakage errors considerably. Calculations for a few drainage basins in North America having areas ranging from 2.2×10^5 to 1.4×10^6 km^2, indicate that surface-mass change signals, spatially correlated at length scales of about 200 km, can be retrieved using an averaging kernel which has been smoothed with a Gaussian filter to an accuracy of 10–40% of the signal amplitude plus <1 cm satellite measurement error. Using the Lagrange multiplier minimization method reduces the amount of leakage error by about half, so that mass anomalies can be computed to an accuracy of 5–20% of the signal amplitude plus <1 cm satellite measurement error. Surface-mass change signals spatially correlated at longer length scales can be retrieved with almost no leakage error and satellite errors of less than a few millimeters.

Appendix A: Inversion With Arbitrary Covariance Functions

[35] While more complicated than the case of an azimuthally symmetric covariance function, it is possible to use the full signal and satellite error covariance matrices to construct an optimized averaging kernel. Beginning with (36), $\overline{W}$, ϑ, and σ are replaced with their respective spherical harmonic expansions. The variance of the leakage becomes

$$\begin{aligned}\mathrm{var}(\varepsilon_{lkg}) = \sum_{l,m}\sum_{l',m'} &\left(W^c_{lm} - \vartheta^c_{lm}\right)\left(W^c_{l'm'} - \vartheta^c_{l'm'}\right)\Gamma^{cc}_{ll'mm'} \\ &+\left(W^c_{lm} - \vartheta^c_{lm}\right)\left(W^s_{l'm'} - \vartheta^s_{l'm'}\right)\Gamma^{cs}_{ll'mm'} \\ &+\left(W^s_{lm} - \vartheta^s_{lm}\right)\left(W^s_{l'm'} - \vartheta^s_{l'm'}\right)\Gamma^{ss}_{ll'mm'} \\ &+\left(W^s_{lm} - \vartheta^s_{lm}\right)\left(W^c_{l'm'} - \vartheta^c_{l'm'}\right)\Gamma^{sc}_{ll'mm'} \end{aligned} \quad (A1),$$

where $\Gamma_{ll'mm'}$ are the covariance matrices of the signal:

$$\Gamma^{cc}_{ll'mm'} = \frac{1}{n}\sum_{i=1}^{n}\sigma^c_{lm}(t_i)\sigma^c_{l'm'}(t_i),\ etc. \quad (A2)$$

The variance of the basin-averaged satellite measurement errors is

$$\begin{aligned}\mathrm{var}(\varepsilon_{sat}) = \sum_{l,m}\sum_{l',m'} K_l K_{l'}\big[&W^c_{lm}W^c_{l'm'}\Lambda^{cc}_{ll'mm'} + W^c_{lm}W^s_{l'm'}\Lambda^{cs}_{ll'mm'} \\ &+ W^s_{lm}W^s_{l'm'}\Lambda^{ss}_{ll'mm'} + W^s_{lm}W^c_{l'm'}\Lambda^{sc}_{ll'mm'}\big],\end{aligned} \quad (A3)$$

where $\Lambda_{ll'mm'}$ are the covariance matrices of the GRACE measurement errors (see equations (9)–(12)).

A1. Minimization of Total Error

[36] Let

$$\overline{\vartheta} = \begin{bmatrix}\vartheta^c_{lm}\\ \vartheta^s_{lm}\end{bmatrix},\ \overline{W} = \begin{bmatrix}W^c_{lm}\\ W^s_{lm}\end{bmatrix}, \quad (A4)$$

$$\overline{\overline{\Gamma}} = \begin{bmatrix}\Gamma^{cc}_{ll'mm'} & \Gamma^{sc}_{ll'mm'}\\ \Gamma^{cs}_{ll'mm'} & \Gamma^{ss}_{ll'mm'}\end{bmatrix},\ \overline{\overline{\Lambda}} = \begin{bmatrix}K_lK_{l'}\ \Lambda^{cc}_{ll'mm'} & K_lK_{l'}\ \Lambda^{sc}_{ll'mm'}\\ K_lK_{l'}\ \Lambda^{cs}_{ll'mm'} & K_lK_{l'}\ \Lambda^{ss}_{ll'mm'}\end{bmatrix} \quad (A5)$$

Then

$$\mathrm{var}(\varepsilon_{lkg}) = \left(\overline{\vartheta} - \overline{W}\right)^T\ \overline{\overline{\Gamma}}\ \left(\overline{\vartheta} - \overline{W}\right) \quad (A6)$$

$$\mathrm{var}(\varepsilon_{sat}) = \overline{W}^T\ \overline{\overline{\Lambda}}\ \overline{W}. \quad (A7)$$

To find the averaging kernel coefficients which minimize the total error, we set the gradient with respect to $\overline{W}$ of the sum of the error variances to zero,

$$\overline{\nabla}_W\left[\left(\overline{\vartheta} - \overline{W}\right)^T\ \overline{\overline{\Gamma}}\ \left(\overline{\vartheta} - \overline{W}\right) + \overline{W}^T\ \overline{\overline{\Lambda}}\ \overline{W}\ \right] = 0, \quad (A8)$$

which produces

$$\left[\overline{\overline{\Gamma}} + \overline{\overline{\Lambda}}\right]\ \overline{W} - \overline{\overline{\Gamma}}\ \overline{\vartheta} = 0. \quad (A9)$$

Equation (A9) is a linear system, which can be solved numerically for $\overline{W}$.

A2. Lagrange Multiplier Method

[37] As an alternative to equation (A6) we may define the leakage as the ratio of the spatial variance of the difference between the exact and approximate averaging kernels to that of the exact averaging kernel,

$$\begin{aligned}\mathrm{var}\left(\varepsilon_{lkg}\right) &= \frac{\int\left[\overline{W}(\theta,\phi) - \vartheta(\theta,\phi)\right]^2\ d\Omega}{\int\left[\vartheta(\theta,\phi)\right]^2\ d\Omega} \\ &= \frac{1}{4\ \pi\Omega_{\mathrm{region}}}\left(\overline{\vartheta} - \overline{W}\right)^T\ \left(\overline{\vartheta} - \overline{W}\right).\end{aligned} \quad (A10)$$

This definition of leakage is free from the assumptions regarding the form of the expected signal required by equation (A6). However, those assumptions provided a means of directly comparing leakage error to satellite error. In the absence of such a connection, one cannot minimize

the total error. Instead, one may use a Lagrange multiplier technique to minimize either leakage error or satellite error, subject to a constraint on the other type of error. Denoting the Lagrange multiplier by λ, we determine the values of $\overline{W}$ and λ that minimize the quantity

$$\xi = \left(\overline{\vartheta} - \overline{W}\right)^T \left(\overline{\vartheta} - \overline{W}\right) + \lambda \left\{\overline{W}^T \,\overline{\overline{\Lambda}}\, \overline{W} - \Delta^2\right\}, \qquad \text{(A11)}$$

where Δ^2 is the desired variance of the satellite measurement errors, averaged over the basin. The $4\pi\Omega_{\text{region}}$ in equation (A10) has been absorbed into λ. Setting the gradient of ξ with respect to $\overline{W}$ equal to zero gives

$$\left[\overline{\overline{I}} + \lambda\, \overline{\overline{\Lambda}}\,\right] \overline{W} = \overline{\vartheta}, \qquad \text{(A12)}$$

where $\overline{\overline{I}}$ is the identity matrix. Setting the partial derivative of ξ with respect to λ equal to zero returns the requirement that $\text{var}(\varepsilon_{sat}) = \Delta^2$, which can be combined with to give an equation for λ

$$\text{var}(\varepsilon_{sat}) = \overline{\vartheta}^T \left[\overline{\overline{I}} + \lambda\, \overline{\overline{\Lambda}}\,\right]^{-1\,T} \overline{\overline{\Lambda}} \left[\overline{\overline{I}} + \lambda\, \overline{\overline{\Lambda}}\,\right]^{-1} \overline{\vartheta}, \qquad \text{(A13)}$$

Once λ is known, it can be used with equation (A12) to solve for $\overline{W}$.

[38] This method can also be applied to the converse of this problem: minimizing satellite error for a given value of leakage. In this case, equation (A12) still describes the averaging kernel coefficients. However, λ is determined now by solving

$$\overline{\vartheta}^T \left[\overline{\overline{I}} - \left[\overline{\overline{I}} + \lambda\, \overline{\overline{\Lambda}}\right]^{-1}\right]^T \left[\overline{\overline{I}} - \left[\overline{\overline{I}} + \lambda\, \overline{\overline{\Lambda}}\right]^{-1}\right] \overline{\vartheta} = R\, 4\pi\Omega_{\text{region}}, \qquad \text{(A14)}$$

where R is the desired ratio of the spatial variances (equation (A10)).

[39] **Acknowledgments.** We wish to thank Steven Jayne and Isabella Velicogna for their helpful discussions. With the assistance of Lynda Lastowka, the river basin boundaries were extracted from the HYDRO 1K Elevation Derivative Database maintained by the U.S. Geological Survey EROS Data Center from their web site at http://edcdaac.usgs.gov/gtopo30/hydro/. This work was partially supported by NASA grants NAG5-9450 and NAG5-7703 to the University of Colorado, by a CIRES Innovative Research Grant, and a NASA Earth Systems Science Fellowship awarded to Sean Swenson.

References

Cayan, D., and K. Georgakakos, Hydroclimatology of continental watersheds, *Water Resour. Res.*, *31*(3), 677–697, 1995.

Chao, B. F., and R. S. Gross, Changes in the Earth's rotation and low-degree gravitational field induced by earthquakes, *Geophys. J. R. Astron. Soc.*, *91*, 569–596, 1987.

Entin, J., A. Robock, K. Vinnikov, S. Hollinger, S. Liu, and A. Namkhai, Temporal and spatial scales of observed soil moisture variations in the extratropics, *J. Geophys. Res.*, *105*(D9), 11,865–11,877, 2000.

Jekeli, C., Alternative methods to smooth the Earth's gravity field, *Rep. 327*, Dep. of Geod. Sci. and Surv., Ohio State Univ., Columbus, 1981.

Jet Propulsion Laboratory, GRACE Science and Mission Requirements Document, GRACE 327-200, Rev. D, *JPL Publ. D-15928*, 2001.

Rodell, M., and J. Famiglietti, An analysis of terrestrial water storage variations in Illinois with implications for GRACE, *Water Resour. Res.*, *37*, 1327–1339, 2001.

Swenson, S., and J. Wahr, Estimated effects of the vertical structure of atmospheric mass on the time-variable geoid, *J. Geophys. Res.*, *107*, 10.1029/2000JB000024, in press, 2002.

Velicogna, I., J. Wahr, and H. van den Dool, Can surface pressure be used to remove atmospheric contributions from GRACE data with sufficient accuracy to recover hydrological signals?, *J. Geophys. Res.*, *106*(B8), 16,415–16,434, 2001.

Vinnikov, K., A. Robock, N. Speranskaya, and C. Schlosser, Scales of temporal and spatial variability of midlatitude soil moisture, *J. Geophys. Res.*, *101*(D3), 7163–7174, 1996.

Wahr, J., M. Molenaar, and F. Bryan, Time variability of the Earth's gravity field: Hydrological and oceanic effects and their possible detection using GRACE, *J. Geophys. Res.*, *103*(B12), 30,205–30,229, 1998.

S. Swenson and J. Wahr, Department of Physics and Cooperative Institute for Research in Environmental Sciences, University of Colorado, Campus Box 390, Boulder, CO 80309-0390, USA. (swensosc@colorado.edu; wahr@lemond.Colorado.edu)